JCI insight

Time-restricted feeding reduces cardiovascular disease risk in obese mice

Paramita Pati, … , David M. Pollock, Jennifer S. Pollock

JCI Insight. 2025. https://doi.org/10.1172/jci.insight.160257.

Research In-Press Preview Nephrology

Graphical abstract

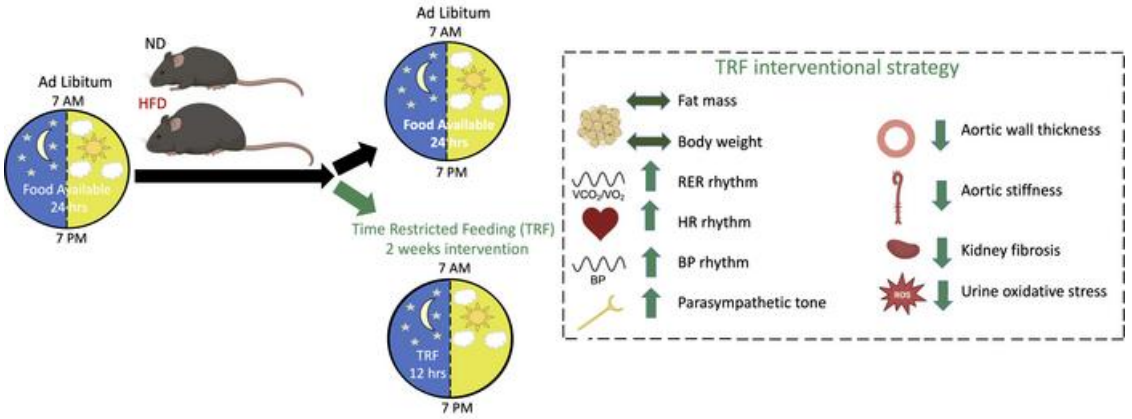

Find the latest version:

https://jci.me/160257/pdf

Time-restricted feeding reduces cardiovascular disease risk in obese mice

Paramita Pati, [*1] Carmen De Miguel,[*1] Jodi R. Paul,[2] Dingguo Zhang,[1] Jackson Colson,[1] John Miller Allan,[1] Claudia J. Edell,[1] Megan K. Rhoads,[1] Luke S. Dunaway,[1] Sara N. Biswal,[1] Yihan Zhong,[1] Randee Sedaka,[1] Telisha Millender-Swain,[3] Shannon M. Bailey,[3] Karen L. Gamble,[2] David M. Pollock,[1] and Jennifer S. Pollock[1]

[1]Cardio-Renal Physiology & Medicine, Division of Nephrology, Department of Medicine, [2]Division of Behavioral Neurobiology, Department of Psychiatry, [3]Division of Molecular and Cellular Pathology, Department of Pathology, Heersink School of Medicine, University of Alabama at Birmingham, Birmingham, AL

*Denotes co-first authors with equal contributions

Corresponding author: Jennifer S. Pollock, PhD

Cardio-Renal Physiology and Medicine

Division of Nephrology, Department of Medicine

University of Alabama at Birmingham

McCallum Research Building 515

Birmingham, AL 35233

Phone: 205-975-7525

Email: jenniferpollock@uabmc.edu

Conflict-of-interest statement: The authors have declared that no conflict of interest exists.

List of incorporated changes for publication:

1. Reduced word count to less than 12,000 words.
2. Revised title length to 9 words.
3. Confirmed all author names are correct and complete.
4. Author contributions revised to include the method used to assign authorships for co-first authors.
5. Ensured all protein and gene symbols are formatted correctly.
6. Verified that any novelty statements were removed or qualified.
7. Verified that all statements of significance refer only to statistical significance.
8. Confirmed that the study does not include any gifts of materials.
9. Confirmed Data availability section at end of methods includes statement about available supporting data values file in supplement.
10. Confirmed that only commercial antibodies were used with source and catalog number included.
11. Ensured that animals used is indicated.
12. Confirmed all references are present without duplication and formatted according to journal style.
13. Confirmed that supporting data values associated with the main manuscript and supplement material are included in a single excel file with tabs for all figures.
14. Verified that supplement is in final version.
15. Verified that all figures are prepared according to journal style.

Abstract

Disrupted feeding and fasting cycles as well as chronic high fat diet (HFD)-induced obesity are associated with cardiovascular disease risk factors. We designed studies that determined whether two weeks of time-restricted feeding (TRF) intervention in mice fed a chronic HFD would reduce cardiovascular disease risk factors. Mice were fed a normal diet (ND; 10% fat) *ad libitum* or HFD (45% fat) for 18 weeks *ad libitum* to establish diet-induced obesity. ND or HFD mice were continued on *ad libitum* diet or subjected to TRF (limiting food availability to 12 hr only during the dark phase) during the final two weeks of the feeding protocol. TRF improved whole-body metabolic diurnal rhythms without a change in body weight. HFD mice showed reduced blood pressure dipping compared to ND, which was restored by TRF. Further, TRF reduced aortic wall thickness, decreased aortic stiffness, as well as increased kidney tubular brush border integrity, decreased renal medullary fibrosis, and reduced renal medullary T cell inflammation in HFD mice. These findings indicate that TRF may be an effective intervention for improving vascular and kidney health in a model of established diet-induced obesity.

Introduction

Feeding-fasting cycles influence the development of metabolic and vascular disease in humans (1) as well as physiological homeostasis (2, 3). Changes in a regular light-dark cycle and feeding-fasting cycles, lead to neural and endocrine homeostatic dysfunction (4-7). For example, mice fed an *ad libitum* high fat diet (HFD) have higher levels and altered rhythms of glucose and leptin, which are important metabolic regulators (7). Chronic *ad libitum* HFD mediates both aortic and kidney damage (6, 8-11) as well as contributing to the development of cardiometabolic disease (8-11).

Blood pressure and vascular function display diurnal rhythms (12-14) that are important for cardiovascular health. Loss of blood pressure dipping is closely associated with target organ damage and cardiovascular disease (15). Both endothelial function and vascular resistance display light-dark variation in animal models (16, 17) and humans (13, 14), with endothelium-dependent relaxation as well as vascular resistance peaking during the active period (14, 16-18). HFD leads to endothelial dysfunction with loss of endothelial NO signaling in mice (19-21). Similarly, humans consuming a HFD have reduced endothelial function and increased cardiovascular disease risk (19, 22, 23). However, it is unknown whether feeding-fasting cycles with a HFD influence these cardiovascular disease risk factors.

Recent studies demonstrate the beneficial effects of time-restricted eating or feeding (TRF) on cardiometabolic health in humans and animals (24-35). In contrast to caloric restriction, TRF limits food intake to a specific time window but not the food content thus induces increased fasting without reducing daily total caloric intake (36). Chronic TRF coincident with high fat feeding reduces metabolic disease in rodents (30-35). In humans, TRF improves glucose levels, insulin sensitivity, cholesterol, oxidative stress, and blood pressure (24-29) with food intake restricted to a daily time window without caloric restriction, suggesting that the timing of food intake and fasting is critical in the advancement and progression of disease.

We hypothesized that restricting food availability to the dark phase for a short intervention in a murine model of established diet-induced obesity would improve cardiovascular disease risk factors, specifically restore blood pressure dipping, decrease kidney damage as well as increase aortic

endothelial function and reduce aortic wall thickness and stiffness. To address this hypothesis, 8-week-old mice were fed *ad libitum* normal diet or HFD for 18 weeks followed by 2 weeks of *ad libitum* or TRF (food available only during the 12-h dark phase) for a total of 20 weeks housed under similar conditions except for the food availability. During the final few days of the study, we measured metabolic rhythms, hemodynamics, diurnal aortic vascular reactivity, aortic and kidney pathology, and circulating mediators in all four diet and feeding groups. The results indicate that 2 weeks of TRF in a mouse model of established HFD-induced obesity is sufficient to reduce cardiovascular disease risk and improve vascular health compared to *ad libitum* HFD independent of body weight.

Results

TRF reinstates whole body metabolic rhythms independent of weight gain in HFD fed mice. Mice fed a normal diet (ND) or HFD were subjected to 18 weeks of *ad libitum* feeding, followed by 2 weeks with food available *ad libitum* in the control groups or only during the 12-h dark phase in the TRF groups (Figure 1A) for a total of 20 weeks feeding protocol. Sham control mice were housed alongside the TRF mice and were exposed to the same disturbance by lab personnel at specific times of day, including having their cage and food container similarly handled as the TRF mice except that food remained in the container, thus controlling for any confounders related to the TRF protocol. Mice on HFD had significantly higher body weights than mice on ND (Figure 1B, 1D). Most mice in this study were group housed in home cages with subsets of mice singly housed for specific measurements. Interestingly, body weight was not affected by the 2-week TRF period in both diet groups of mice in group housed home cages or in singly housed specialty cages (Figure 1B, 1C, 1D; Supplemental Figure 1). Quantitative magnetic resonance measurements revealed significantly higher fat mass in mice on HFD compared to ND groups regardless of TRF (Figure 1E). Lean mass was also significantly higher in HFD+TRF mice (Figure 1F). Measurements of food consumption during the 12 hr light and dark phase were monitored during the final 3 days of the dietary and feeding protocol after an acclimation period with mice in the singly housed metabolic cages. There is an obvious difference in the food consumption during the light period in the TRF groups of both diets compared to the *ad libitum* groups (Figure 1G) since there is no food available in the light period for the TRF groups. Food consumption during the dark phase did not significantly differ among the four dietary and feeding groups of mice although there is a trend for the HFD groups to consume less food (Figure 1G). Daily (24-hr) food and caloric intake was monitored in both the singly housed metabolic cages as well as in group housed home cages. TRF did not influence the daily food intake or the daily caloric intake in either diet group in the singly housed cages (Supplemental Figure 2). Mice on HFD in home cages showed significantly decreased daily food intake but not caloric intake compared to the ND mice in home cages (Supplemental Figure 2). TRF did not influence daily food intake or caloric intake in ND

mice in home cages (Supplemental Figure 2). TRF significantly increased daily food intake and caloric intake in HFD mice in home cages (Supplemental Figure 2).

We examined the whole-body respiratory exchange ratio (RER) profile continuously over 24-h to determine whether TRF would improve this metabolic rhythm (Figure 1I). RER is a ratio of VO_2 to CO_2 and as such is not normalized to body weight or composition. ND mice displayed a diurnal variation in RER (P = 0.004; Figure 1I, 1J) as expected. While HFD mice showed no difference in RER between light and dark phases (Figure 1I, 1J). Surprisingly, TRF significantly increased the RER light-dark difference in both ND and HFD mice (ND, P < 0.001; HFD, P < 0.001; Figure 1I, 1J). Energy expenditure normalized to lean body mass was significantly higher in HFD compared to ND mice (main effect of diet, P = 0.005; Figure 1K), and TRF increased the energy expenditure light-dark difference in both ND and HFD mice (time of day × time of feeding interaction, P = 0.002; Figure 1K). Resting metabolic rate (RMR) normalized to lean body mass was significantly higher in HFD mice compared to ND mice (main effect of diet, P < 0.001) with a trend toward decreased RMR with TRF in ND and HFD mice (main effect of time of feeding, P = 0.058; Figure 1L).

TRF improves blood pressure (BP) and heart rate (HR) dipping and rhythms. We sought to examine whether TRF would improve BP in HFD mice. BP follows a well-established diurnal rhythm of lower BP during the light phase compared to the dark phase in mice (Figure 2, Supplemental Table 1). We found that the chronic HFD blunted mean arterial pressure (MAP), systolic blood pressure (SBP), and diastolic blood pressure (DBP) dipping compared to ND mice (Figure 2A-2F). TRF reinstated MAP, SBP, and DBP dipping in ND and HFD mice (Figure 2A-2F; ΔMAP: ND, 17 ± 1.0 mmHg; ND+TRF, 20 ± 2.1 mmHg; HFD, 15 ± 1.2 mmHg; HFD+TRF, 19 ± 0.9 mmHg; n = 6–8). Cosinor analysis of BP rhythms confirmed these results showing that TRF increases the amplitude of MAP, SBP, and DBP without changes in mesor or acrophase in the HFD mice (Supplemental Table 1).

Diurnal variation in HR was observed in all groups, however HFD mice show increased HR during both light and dark phases (Figure 2G, 2H). TRF significantly reduced HR in ND and HFD mice during the light phase (P = 0.008; Figure 2G, 2H). TRF also increased the light-dark HR difference

(ΔHR: ND, 70 ± 4.7 bpm; ND+TRF, 94 ± 9.1 bpm; HFD, 74 ± 9.5 bpm; HFD+TRF, 119 ± 10.3 bpm; n = 6–8; Two-way ANOVA results: Time of feeding, $P < 0.01$; HFD vs. HFD+TRF, $P = 0.007$).

Time domain analysis of HR variability revealed that time of day, diet, and time of feeding altered beat-to-beat interval (N-N interval) (Supplemental Table 2). The standard deviation of the N-N interval (SDNN) was lower in HFD mice compared to ND mice, with TRF improving the light-dark difference in SDNN in a time-of-day-dependent manner independent of dietary fat content. The root mean of SDDN (RMSSD; reflecting vagal mediation of heart rate variability) was also lower in HFD than ND mice and was improved during the light phase by TRF, although not restored to the level observed in ND mice. The % of N-N intervals exceeding 6 msec (pNN_6) was also lower in HFD mice.

Locomotor activity measured by telemetry displayed a diurnal rhythm in all 4 groups of mice being highest in the dark phase as expected (Figure 2I). Mice eating a HFD displayed lower locomotor activity than mice on ND. TRF significantly increased activity in ND mice with no change in HFD mice (Figure 2I, 2J). The light-dark difference in activity was significantly increased in ND+TRF mice (Δ Activity: ND, 5.7 ± 1.0 counts/min; ND+TRF, 10.2 ± 1.1 counts/min; HFD, 4.3 ± 0.6 counts/min; HFD+TRF, 4.4 ± 0.3 counts/min; n = 6–8; Two-way ANOVA results: Diet, $P < 0.01$; Time of feeding, P = 0.01; Interaction, $P = 0.02$; ND vs. ND+TRF, $P = 0.006$). Patterns of locomotor activity appeared to be similar among ND, HFD, and HFD+TRF mice, as shown in representative actograms (Figure 2K). Interestingly, TRF significantly increased food anticipatory activity in ND mice compared to HFD mice (Figure 2L).

TRF restores aortic function and reduces aortic wall thickness in HFD fed mice. Endothelium-dependent and -independent vasorelaxation were assessed in thoracic aorta isolated during both light and dark phases (ZT0 and ZT12) based on responses to acetylcholine (Ach) and sodium nitroprusside (SNP), respectively (Figure 3A, 3B; Table 1). Endothelium-independent relaxation, assessed by the NO donor SNP, was similar in all groups during both the light and dark phases (Table 1), indicating that the endothelium is specifically impaired by this model of chronic HFD. Endothelial function was similar in ND and ND+TRF mice. In HFD mice, Ach-mediated vasorelaxation

were significantly reduced in the light compared to the dark phase ($p < 0.001$; Figure 3C). In general, Ach-induced maximum vasorelaxation (E_{max}) was significantly impaired in ad lib-fed HFD mice compared to ND mice ($p = 0.006$) and tended to be improved by TRF ($p = 0.061$; Figure 3C). Sensitivity to Ach ($logEC_{50}$) showed a light-dark difference although no effects of diet or time of feeding were observed (Figure 3D).

We also determined aortic vasoconstriction responses to PE and KCl during the light and dark phases (Figure 3E, 3F; Table 1). In ND mice, PE-induced vasoconstriction was greater during the dark compared to the light phase (Figure 3G). The diurnal difference of PE-induced vasoconstriction was maintained in all groups of mice, as time of day had a significant main effect (Figure 3G); however, TRF of HFD mice increased sensitivity to PE-induced vasoconstriction during the light phase (Figure 3H). KCl-induced vasoconstriction was not different among groups (Table 1).

Aortic pulse wave velocity (PWV), a determinant of aortic function, was also assessed in the four groups of mice. PWV is a measure of aortic stiffness. Aortic stiffness, an indicator of cardiovascular disease, and known to be highly associated with obesity. We found that aortic PWV was significantly higher in HFD mice than in ND mice (Figure 3I). TRF restored the PWV in HFD mice to that observed in ND mice. Aortic PWV was similar between ND and ND+TRF mice (Figure 3I). We also determined whether TRF would impact aortic wall thickness and fibrosis in HFD mice (Figure 3J, 3K, 3M, 3N). Aortic wall thickness was significantly increased in HFD mice compared to ND mice. A significant interaction between diet and time of feeding was also observed, largely driven by lower wall thickness in the HFD+TRF group (Figure 3J). Neither dietary fat nor time of feeding altered the extent of aortic fibrosis apparent among the different groups of mice (Figure 3K). Similarly, we did not find changes in Type I and III collagen content assessed by Picrosirius red staining among groups (Figure 3L, 3O, 3P).

TRF improves kidney pathology in HFD mice. Reduced BP dipping is an indicator of target organ damage. Kidney damage is also a consequence of diet-induced obesity; thus, we sought to determine the effect of TRF on kidney pathology. Chronic *ad libitum* HFD induced fibrotic deposition in the vasa recta vascular beds of the kidney medulla (Figure 4A, 4B). In addition, TRF reduced type I and

III collagen deposition in the medulla of HFD mice (Figure 4C, 4D, 4E) and reduced outer medullary fibronectin mRNA expression (Interaction, $P = 0.0513$; Figure 4F) in HFD mice. Histological assessments verified that, compared to ND mice, chronic HFD mice exhibited renal cortical damage evidenced by the appearance of vacuoles in proximal tubular cells, proximal tubule dilation, and the presence of glomerulosclerosis (Figure 4G, 4H, 4I, 4J, 4K) as well as decreased proximal tubular brush border integrity (Figure 4L, 4M). TRF normalized proximal tubular brush border integrity (Figure 4L, 4M) and tended to reduce the abundance of proximal tubule vacuoles (Figure 4G, 4H). However, TRF did not improve glomerulosclerosis in HFD mice (Figure 4J, 4K).

Assessment of renal immune cell infiltration revealed that HFD mice had significantly elevated numbers of $CD3^+$ cells (T lymphocytes) within the medullary vasa recta region compared to ND mice. TRF significantly reduced T lymphocytes in HFD mice (Figure 4N, 4O). However, $F4/80^+$ (macrophage) cell numbers in this same region did not differ significantly among the 4 groups of mice although the TRF groups were generally lower than ad lib fed mice (Figure 4P, 4Q).

To further assess HFD-induced kidney injury, urinary excretion of the damage markers neutrophil gelatinase-associated lipocalin (NGAL), kidney injury marker 1 (KIM-1), and albumin were measured during the light and dark phases. NGAL excretion showed a day-night difference that was higher during the dark phase in *ad lib*-fed HFD mice (Figure 4R). TRF evoked similar reductions in dark-phase KIM-1 excretion by both diet groups (Figure 4S). Urinary albumin excretion was significantly higher during the dark phase but did not differ among groups (Figure 4T). HFD mice had significantly higher urinary excretion of the oxidative stress marker, hydrogen peroxide (H_2O_2), during the dark phase compared to the light phase (Figure 4U). Urinary excretion of the DNA damage product 8-hydroxy 2-deoxyguanosine (8-OHdG) was significantly reduced by TRF in HFD mice during the dark phase (Figure 4V). TRF did not influence diurnal water intake, urine output, or electrolyte excretion by HFD mice (Supplemental Table 3).

TRF alters rhythms of plasma hormones, metabolites, and adipokines. We performed additional analyses of circulating factors known to be important contributors to obesity-dependent

cardiometabolic dysfunction, utilizing a cohort of mice with blood collections every 4 hours. Insulin-like growth factor 1 (IGF1) is a liver-derived hormone with insulin-like effects (37) and also affects vascular function. Plasma IGF1 levels were arrhythmic in *ad libitum* ND and HFD mice, whereas TRF mice showed rhythmicity (Supplemental Figure 3A; Supplemental Table 4). IGF1 rhythms in TRF mice on HFD and ND were antiphase to each other, with HFD+TRF peaking in the light phase and ND+TRF peaking in the dark phase (Supplemental Table 4). The ketone body metabolite, beta hydroxybutyrate (BHB), is mainly derived from fatty acids in the liver and is important for energy metabolism in extra-hepatic tissues(38). Circulating levels of BHB were not significantly different between groups and were higher during the dark phase (Supplemental Figure 3B; Supplemental Table 4). Plasma BHB levels were rhythmic in all diet groups except the ND+TRF group. HFD shifted the phase of BHB compared to ND, but rhythms were similar in HFD and HFD+TRF mice (Supplemental Table 4). Non-esterified fatty acids (NEFA) are metabolites that are positively associated with vascular and organ damage in models of diet-induced obesity(11). Plasma NEFA concentrations were rhythmic in ND, ND+TRF, and HFD+TRF mice, but were arrhythmic in *ad libitum* HFD mice (Supplemental Figure 3C; Supplemental Table 4). TRF significantly shifted the NEFA phase in ND mice (Supplemental Table 4).

Plasma concentration of nitrite (an NO metabolite) has been shown previously to reflect endothelial function acutely(19-21, 39, 40). In contrast, plasma nitrate levels are known to reflect dietary nitrate intake(41, 42). Thus, we measured plasma nitrite and nitrate levels from a cohort of mice with blood collections every 4 h. Plasma nitrite was arrhythmic in all groups of mice, while plasma nitrate was rhythmic in ND+TRF and HFD+TRF mice (Supplemental Figure 3D, 3E; Supplemental Table 4).

We measured markers of kidney function in plasma at 4-h intervals over a 24-h period. The results (Supplemental Figure 3F, 3G; Supplemental Table 5) reveal that blood urea nitrogen (BUN) levels were similar across the 4 dietary and feeding groups and were arrhythmic in all groups of mice. Plasma creatinine levels were also similar among all 4 dietary and feeding groups but rhythmic only in HFD mice.

Adipokines (adipose-derived factors such as adiponectin and leptin) have key metabolic roles and were previously shown to have direct effects on the vasculature, particularly on the endothelium(43-51). Plasma adiponectin concentration was unchanged across all groups during the light and dark phase, although a time-of-day × time-of-feeding interaction was significant (Supplemental Figure 4A). Plasma leptin levels were significantly higher in *ad libitum* HFD and HFD+TRF mice compared to ND mice at ZT1, ZT5, ZT12, and ZT17 while TRF significantly decreased leptin only at ZT12 in HFD mice (Supplemental Figure 4B). There were significant main effects of diet, time of feeding, and time of day as well as significant interactions of time of day × diet and diet × time of feeding.

Plasma levels of the lipid peroxidation biomarker 8-isoprostane was measured to assess oxidative stress in HFD and HFD+TRF mice during the light (ZT5) and dark (ZT12) phase. TRF trended to reduce 8-isoprostane in HFD mice at ZT5 compared to HFD+TRF mice at ZT12 (Supplemental Figure 5A); however, the DNA damage product 8-OHdG was not affected by time of feeding or time of day in plasma from HFD mice (Supplemental Figure 5B).

Discussion

Here we show significant evidence that a short-term TRF intervention reduces the cardiovascular disease risk in a mouse model of established diet-induced obesity. The major findings of this study demonstrate that 2 weeks of TRF in an established model of diet-induced obesity: 1) does not reduce body weight, 2) improves whole-body energy metabolic rhythms, 3) restores BP and HR dipping, 4) restores aortic PWV, reduces aortic wall thickness improving aortic health, and 5) abrogates renal proximal tubular injury, reduces kidney medullary fibrosis and collagen content, as well as kidney T cell infiltration improving kidney health. These exciting results complement clinical data suggesting significant TRF-induced benefits to reduce cardiovascular disease risk factors in obesity and that TRF may be an effective intervention for improving health in obesity.

***TRF, cardiometabolic rhythms, and BP rhythms*.** We examined whole body metabolic rhythms in this obesity model and found that *ad libitum* consumption of 45% HFD abolished circadian changes in the RER compared to mice fed a ND. Our findings show TRF improved RER light vs. dark difference in both ND and HFD mice similar to a previous study in which mice were fed a 61% fat HFD and subjected to dark phase 8-h TRF for at least 12 weeks (31). Previous studies in mice on a chronic ≥ 60% HFD, with TRF maintained throughout the duration of HFD feeding for 20 weeks, showed that TRF protected against hepatic steatosis and reduced insulin resistance as well as altered glucose metabolism and lipid homeostasis (32). The current study demonstrates that 2 weeks of TRF intervention is sufficient to improve whole body metabolic diurnal rhythms in mice that had been fed a HFD *ad libitum* for a prolonged (20 week) period.

Normal BP and HR rhythms show a decrease or “dip” during the light phase in rodents. In the present study, we found that this chronic HFD model leads to significantly reduced dipping of BP and HR compared to ND mice, with TRF restoring BP and HR dipping in HFD mice to levels similar to those of ND mice. Prior studies of mice fed a 60% HFD for periods ranging from 8 weeks to 16 months found a modest increase or no change in BP and/or HR (52-55). In another model characterized by obesity,

the leptin receptor-deficient *db/db* mouse, BP dipping is reduced along with an elevated 24-h BP (56, 57). Type II diabetes in humans is also associated with disrupted diurnal BP variation (58, 59). Our analysis of HR variability suggests that TRF in HFD mice may improve parasympathetic tone during the inactive/fasting light period, which is linked to restoration of BP and HR dipping. Importantly, it is well documented that a reduced BP dipping profile increases the risk for hypertension, end-organ damage, and cardiovascular disease in humans (15, 60). Our findings indicate that the feeding-fasting cycle is a critical mediator in systemic cardiovascular rhythms.

TRF and aortic health. Aortic damage, such as increased wall thickness and fibrosis, and aortic stiffness are independent risk factors of hypertension and cardiovascular disease (61, 62). Our focus was to determine whether TRF would mitigate HFD-induced aortic damage and stiffness. As expected, we found that HFD mice have increased aortic medial hypertrophy, or wall thickness, and increased aortic stiffness measured by PWV compared to ND mice. HFD mice exposed to short-term TRF displayed an aortic wall thickness and aortic stiffness measure similar to that seen in ND mice. It is established that the loss of NO bioavailability is linked to aortic damage and stiffness as well as smooth muscle reprogramming (63, 64). However, at this point the TRF-dependent mechanism of reversing aortic remodeling is unclear.

Several studies have demonstrated endothelial dysfunction in rodent models of diet-induced obesity (19, 22, 23). Most studies reported in the literature analyzed endothelial function during the light phase in rodent models, and previous studies with chronic HFD did not determine time-of-day changes in endothelial function (19, 21, 53, 55). Our study assessing vascular reactivity during both the light and dark phases revealed that HFD mice display aortic endothelial dysfunction only during the light phase and that TRF reduces the endothelial dysfunction. Endothelial dysfunction is a mediator of the loss of vascular health (64) and contributes to aortic hypertrophy, fibrosis, and inflammation (65, 66).

Oxidative stress, including increased reactive oxygen species, is an established cause of reduced NO bioavailability leading to endothelial dysfunction in the aorta (67). Isoprostanes, markers of oxidative stress and lipid peroxidation, also contribute to cardiovascular disease (68). A recent study

reported 5 weeks of TRF decreased 8-isoprostane levels in pre-diabetic overweight men that was associated with lower BP (69). Our data in obese male mice suggest that TRF tends to reduce 8-isoprostane in association with restored aortic endothelial function and BP dipping in the light period, possibly mediated by reducing oxidative stress although further research is warranted to decipher this mechanism. HFD mice also had increased aortic stiffness that was normalized by TRF, perhaps due to TRF-mediated decreased oxidative stress. Further research is needed to determine the TRF-induced molecular mechanistic regulation of decreasing oxidative stress.

Previous reports show that plasma nitrite levels are indicative of acute NO activation, and that nitrite and nitrate levels have diurnal variation; however, time-dependent changes in these parameters in animals chronically fed a HFD remained speculative (70). Surprisingly, plasma nitrite concentrations were not rhythmic in any of our groups of mice, suggesting that this is not a robust marker of HFD or TRF-induced changes in endothelial function. Dietary nitrate contributes to the levels of plasma nitrate (71, 72) and our observation that TRF institutes a rhythm in plasma nitrate in both ND and HFD suggests that the timing of food intake affects the level of circulating nitrate.

Endothelial function and vascular contractility show time-of-day-dependent changes under normal dietary conditions with endothelial function lowest when vasoconstriction is highest at the beginning of the active period (16-18). Our study confirms previous reports of a significant time-of-day difference in the total response to adrenergic vasoconstriction in mice fed a ND, with a greater constriction of aortic rings isolated during the dark phase (73, 74). In our study with 45% HFD mice, vasoconstrictor sensitivity of aortic rings to an adrenergic agonist was significantly greater in the dark phase compared to the light phase. Interestingly, TRF increased the sensitivity to adrenergic vasoconstrictor stimuli in HFD mice during the light phase, similar to that seen in the dark phase. Previous reports utilizing mice on a chronic 60% HFD demonstrated blunted aortic vasoconstriction that presumably was assessed during the light phase, although time of day was not specifically stated in the publication(53, 55). Vascular adrenergic activation is a balance of direct stimulation of the smooth muscle adrenergic receptor mediated vasoconstriction and an indirect endothelial alpha2- and beta-

adrenergic receptor-stimulated NO release, with oxidative stress directly influencing this equilibrium (75). At this point, the mechanism for the TRF-induced increased sensitivity to adrenergic stimulation in HFD mice is unclear.

TRF and kidney health. Kidney injury has been observed in obese patients with normal renal function(76), and obesity is a major risk factor for chronic kidney disease and various cardiovascular disorders. We did not observe differences in plasma creatinine or BUN as measures of kidney function in our model, however the present study provides novel data showing that TRF mitigates many of the HFD-induced kidney damage assessments. TRF restored the proximal tubular brush border integrity. Proximal tubules are high energy-demanding cells especially under high fat conditions with increased fatty acid oxidation (77). Previous reports show that HFD promotes proximal tubular damage via oxidative stress (11). TRF prevented the dark phase increase in excretion of the urinary oxidative stress marker 8-OHdG, suggesting that TRF in HFD mice reduces oxidative stress in the kidney. Thus, we propose that TRF may protect against proximal tubular damage via reducing oxidative stress.

Kidney fibrosis is one of the hallmarks of end stage kidney disease and HFD-induced kidney damage (11, 78-80). We found that TRF reversed the HFD-induced medullary vasa recta fibrosis, as well as abolishing the HFD-induced increase in medullary type I and III collagen fibers. In contrast, HFD-induced glomerulosclerosis was unchanged by TRF. The distinct mechanisms of HFD-induced glomerulosclerosis and medullary vasa recta fibrosis are unclear at this point. Endothelial cells in the kidney medullary vasa recta are highly specialized and distinct from endothelial cells of the glomeruli and large arteries, both of which respond to environmental stimuli via disparate mechanisms (81).

HFD-induced kidney damage is also mediated by the activation and/or infiltration of immune cells such as macrophages and T cells (52, 79, 82). We saw no difference in the numbers of macrophages ($F4/80^+$) in the four groups of mice, although specific subtypes of macrophages and the activation status were not determined. In contrast, TRF reduced the HFD-induced increase in T cell ($CD3^+$) numbers within the renal medullary vasa recta region associated with the amelioration of fibrosis in the same region. We propose that TRF blocks the increased T cell infiltration and/or

endothelium dysfunction in the kidney medullary vasa recta. Future studies are needed to determine the specific subtypes of immune cells responsive to TRF and potential mechanisms of T cell infiltration.

We examined urinary markers of kidney injury in all four groups of mice. Urine albumin is a marker of kidney glomerular injury used in many investigations. Our model of HFD did not increase albumin or KIM-1 excretion compared to mice on ND, although we found greater glomerulosclerosis and loss of brush border integrity. NGAL excretion is utilized as a biomarker of the severity of kidney injury as it is released and excreted by injured or inflamed kidney tubular cells and immune cells(82, 83). This obesity model also did not show an increase in NGAL excretion compared to ND control mice. However, there was a significant day-night difference in NGAL excretion in HFD mice. These urinary markers of kidney damage appear to not be reflective of the histological changes observed in this obesity model. We propose that further research is needed to decipher obesity-specific urinary kidney damage markers.

Our model employing chronic (20 weeks) feeding of 45% HFD confirmed that the metabolic mediators, IGF1, BHB, NEFA, leptin, and adiponectin, show time-dependent changes. A prior study showed that metabolic mediators, including NEFA and leptin, display disrupted rhythms in mice fed 6 weeks of a chronic 45% HFD (7). IGF1 levels are lower in models of HFD and IGF1 supplementation offers cardioprotection (84). We further observed that timing of feeding-fasting significantly shifted the rhythms of IGF-1 and NEFA predominantly in ND mice. While plasma BHB showed diurnal variation, diet or timing of feeding did not significantly change rhythms. Recently, BHB was shown to lower BP in a model of salt-sensitive hypertension (85). Fasting or reduced caloric intake increases BHB, and humans with obesity-related nonalcoholic fatty liver disease have lower BHB (86, 87). We also observed that leptin levels in HFD mice were increased throughout the light phase and reduced by TRF during the early dark phase. Hatori et al (31) reported that long-term TRF in mice on a 61% HFD lowered leptin following glucose administration or overnight fasting. Leptin is known to have pleiotropic effects regulating cellular metabolism and vascular function, including direct effects on the endothelium, smooth muscle, and immune cells (43-48). Leptin resistance or leptin signaling deficiency observed in

obesity leads to increased cardiovascular disease risk (88) through a plethora of mechanisms. Further investigation is needed to determine whether leptin signaling is directly responsible for the TRF-induced changes in BP, HR, aortic function, and organ damage observed in this study.

In conclusion, the present study demonstrates that a short-term TRF intervention following an established chronic *ad libitum* HFD protocol improves vascular and kidney health. These findings underscore the importance of maintaining behaviors that align with physiological rhythms for maintaining cardiovascular health (89-94) especially in obesity. We anticipate that there is not a sole mechanism driving the TRF-mediated improvements in vascular and kidney health in obesity. These studies provide a wide range of novel and impactful discoveries related to TRF as an intervention in obesity to reduce cardiovascular disease risk factors.

Abbreviated Methods

Full methods are provided in supplemental material.

Sex as a biological variable. Male C57BL/6J mice (Jackson Laboratory, Bar Harbor, ME) were utilized in this study. Our study exclusively examined male mice in this model of diet-induced obesity. It is unknown whether the findings are relevant for female mice.

Animals. Six-week-old male C57BL/6J mice (Jackson Laboratory, Bar Harbor, ME) were provided standard laboratory chow and water ad libitum and kept on a 12 h light:12 h dark cycle (ZT0 = lights on, 7 a.m.; ZT12 = lights off, 7 p.m.) in a temperature and humidity-controlled environment in standard cages that are called “home cages”. Mice were acclimated to this environment for 2-wk before the diet protocols started.

Diet-induced obesity and the TRF intervention protocol. Beginning at 8 weeks of age, male mice were fed *ad libitum* either a normal diet (ND; 10% fat, 3.85 kcal/g; Research Diets, New Brunswick, NJ, catalog #D12450K) or a HFD (45% fat, 4.73 kcal/g; Research Diets, New Brunswick, NJ, catalog #D12451) for 18 weeks. ND and HFD groups were then subjected to TRF or sham intervention for 2 weeks of feeding (from week 18 to week 20). TRF protocol involved research personnel removing food containers to empty the food and replacing empty food containers for 12 h during the dark phase (between ZT12 and ZT0), while the sham protocol involved research personnel removing the food containers and replacing the same containers with replete food. All mice are exposed to the food containers moving in and out. These mice are denoted as ND, ND+TRF or HFD, HFD+TRF throughout the study. Mice were group housed (3 mice/cage) in home cages for the majority of the measurements. Body weight was monitored weekly throughout the feeding protocols in their home cages. Food intake was monitored weekly throughout the protocols and normalized to per mouse with food or caloric intake data reported as g/day and kcal/day. Separate cohorts of mice implanted with telemetry devices were single housed in standard, home cages with TRF proceeding as stated above. CLAMS and metabolic cage studies were performed with separate cohorts of mice that are single housed in the requisite

specialized cages. These mice were acclimated to the cages for 7 days or 3 days prior to the data collection periods, respectively. Mice in specialty cages also proceeded with ad lib or TRF protocols.

Statistics

GraphPad Prism 9 (GraphPad Software Inc., La Jolla, CA) or IBM SPSS Statistics 26 (IBM Corp., Armonk, NY) were used for statistical analysis. Data are represented as mean ± SEM and statistical significance was set at $P<0.05$. Figure legends and table legends indicate specific statistical tests used for each data set. Three-way repeated measures ANOVA was used to compare light and dark phase differences in RER, BP, HR, activity, food intake, water intake, urine production, urinary Na^+ excretion and renal damage markers. Two-way ANCOVA was used for RMR calculated from EE. Body weight, fat mass, lean mass, aortic PWV, QPCR, and histology data were analyzed with two-way ANOVA with Tukey's post hoc test. For telemetry and vascular reactivity data at multiple time points, comparisons were made with three-way ANOVA by Sidak's post hoc test. Two-way ANOVA was used to compare diet and time of feeding during the light or dark period for telemetry and vascular reactivity data. Cosinor analysis of telemetry data was used to assess rhythmic and circadian variables in blood pressure, heart rate, and locomotor activity (117). Cosinor analysis was used to analyze diurnal changes in plasma metabolites, BUN, and creatinine (114). Three-way ANOVA was used to compare plasma adipokine measurements at 4 time points.

Study approval

All animal procedures were approved by the Institutional Animal Care and Use Committee at the University of Alabama at Birmingham and were compliant with the National Institutes of Health *Guide for the Care and Use of Laboratory Animals* (8^{th} ed., National Academy of Sciences, 2011).

Data availability

Data from this paper are provided in the main text or the Supporting Data Values file in the supplement or requests for specific data files should be directed towards the corresponding author.

Author Contributions

PP, CDM, DZ, SMB, KLG, DMP, and JSP conceived and designed research; PP, CDM, DZ, JC, CJE, LSD, TMS, JMA, SNB, YZ, and RS performed experiments; PP, DZ, JRP, CDM, JMA, CJE, MKR, LSD, RS, SMB, KLG, DMP, and JSP analyzed data; PP, DZ, JRP, LSD, CDM, MKR, DMP, SMB, KLG, DMP, and JSP interpreted results of experiments; PP and CDM prepared figures; PP and CDM drafted manuscript; PP, JRP, CDM, LSD, DMP, SMB, KLG, and JSP edited and revised manuscript; all authors approved the final submission. PP and CDM made equal contributions to this research and are co-first authors. PP initiated the study and was identified to be listed first.

PP is currently at the Department of Pharmacology, Medical College of Georgia-Savannah at Georgia Southern Savannah Armstrong Campus, Savannah, GA; LSD is currently at the Berne Cardiovascular Research Center, University of Virginia School of Medicine, Charlottesville, VA; JMA is currently at the Department of Vascular Surgery, Emory University School of Medicine, Atlanta, GA; and, DZ is currently at Montevallo University, Montevallo, AL

Acknowledgements

The authors gratefully acknowledge Dr. Martin Young for his thoughtful discussions in designing these studies. The authors thank Ms. Xiaofen Liu for her outstanding histology expertise. The authors acknowledge the UAB Nutrition Obesity Research Center for conducting QMR measurements in the Small Animal Phenotyping Core funded through the UAB NORC (National Institutes of Health P30DK056336). The authors also acknowledge the UAB Mouse Comprehensive Cardiovascular Core for performing pulse wave velocity measurements. The authors thank the UAB O'Brien Center Core (National Institutes of Health P30 DK 079337) for plasma creatinine measurements.

Sources of Funding

University of Alabama at Birmingham AMC21 Multi-Investigator Grant to SMB, KLG, DMP, and JSP

American Heart Association Grant post-doctoral fellowship 18POST34070051 to PP

National Institutes of Health post-doctoral fellowship 1F32HL146179 to PP

American Heart Association Grant pre-doctoral fellowship 18PRE33990345 to DZ

National Institutes of Health pre-doctoral fellowship F31 DK111067 to RS

National Institutes of Health pre-doctoral fellowship F31 HL149235 to LSD

National Institutes of Health R25DK112731 to JSP in support of JMA

National Institutes of Health K01HL145324 to CDM

National Institutes of Health R21AA026906 to SMB

National Institutes of Health R01NS082413 to KLG

National Institutes of Health R01DK134562 to DMP and JSP

Figure Legends

Figure 1. Time-restricted feeding institutes whole body metabolic rhythms independent of weight gain. (**A**) Experimental design of the dietary protocol depicts 18 weeks of *ad libitum* feeding followed by 2 weeks of *ad libitum* food availability or TRF. (**B**) Longitudinal body weight gain from week 1 to week 18 of ND and HFD followed by week 19 and week 20 of ND (n = 35), ND+TRF (n = 35), HFD (n = 36), and HFD+TRF (n = 36) mice maintained in home cages. (**C**) Change in body weight from week 18 to week 20 from mice maintained in home cages (*P < 0.05, two-way ANOVA). (**D**) Body weights at week 20 in mice maintained in home cages (Two-way ANOVA was used to compare diet and time of feeding). Quantitative magnetic resonance (QMR) measurements of (**E**) Fat mass and (**F**) Lean mass (Two-way ANOVA was used to compare diet and time of feeding, n = 6, *P < 0.05). Food intake was measured during light and dark phases in metabolic cages. Food intake in g/12 h (**G**) and in kcal/12 h (**H**) measured at ZT0 and ZT12. Three-way repeated measures ANOVA was used to compare diet, time of feeding, and time of day (n = 11–12, *P < 0.05). Whole body metabolic rhythms were measured by CLAMS in a separate cohort of mice. Data are shown as the 24-h average profile of (**I**) Respiratory exchange ratio (RER) and (**J**) RER light and dark phase differences. (**K**) Energy expenditure (EE) was determined relative to lean body mass in light and dark phases. Three-way repeated measures ANOVA was used to compare diet, time of feeding, and time of day (n = 6, *P < 0.05). (**L**) Resting metabolic rate (RMR) was calculated. Two-way ANCOVA with lean body mass as the covariate was used (n = 6, *P < 0.05).

Figure 2. TRF improves light phase BP and HR changes. Radiotelemetry was used to measure blood pressure, heart rate, and locomotor activity continuously in unrestrained, conscious mice. Light and dark phases are indicated by white and gray shading, respectively. Telemetry traces of the last 3 days average of (**A**) MAP, (**C**) SBP, (**E**) DBP, (**G**) HR, and (**I**) locomotor activity are shown. Individual mouse BP, HR, and activity for the light and dark phase were assessed by calculating the average from ZT3–ZT10 and ZT15–ZT22 periods, as well as the difference between these periods. Eight-hour averages of light and dark phases with main effects and interactions shown in (**B**), (**D**), (**F**), (**H**), and (**J**). Two-way ANOVA was

used to compare diet and time of feeding during the light or dark period ($^{\dagger}P < 0.05$ ad lib vs. TRF). Three-way repeated measures ANOVA was used to compare diet, time of feeding, and time of day (n = 6–8, $^{*}P < 0.05$). (**K**) Representative actograms of locomotor activity generated with ClockLab (Actimetrics, ClockLab, Wilmette, IL) are shown. Bracket indicates the three days used for analysis in (**A-J**) and (**L**). (**L**) Food anticipatory activity was assessed from telemetry activity data using activity occurring from ZT 8-12 (as percent of total daily activity). Two-way ANOVA was used to compare diet and time of feeding (n = 6–8, $^{*}P < 0.05$).

Figure 3. TRF restores aortic endothelial function and reduces aortic damage in HFD mice. Vascular function studies in thoracic aortae were conducted with cumulative concentration–response curves of Ach, SNP, PE, and KCl. Ach-induced vascular relaxation during the light and dark phases is shown (**A**-**B**), (**C**) E_{max}, and (**D**) $EC_{50.}$ PE-induced vasoconstriction curves in the light and dark phases are shown (**E**-**F**), (**G**) AUC, and (**H**) EC_{50}. Two-way ANOVA was used to compare diet and time of feeding during the light or dark period ($^{\dagger\dagger}P < 0.05$ HFD and HFD+TRF light vs. HFD and HFD+TRF dark). Three-way ANOVA was used to compare diet, time of feeding, and time of day with Sidak's post hoc test (n = 5–10, $^{*}P < 0.05$; $^{£}P < 0.05$ light vs. dark). Main effects and interactions are shown below graphs. (**I**) Aortic stiffness was assessed with pulse wave velocity (PWV) measurements between ZT2–ZT5 in a separate cohort of mice. Two-way ANOVA was used to compare diet and time of feeding (n = 4–12, $^{*}P < 0.05$). A different cohort of mice sacrificed at ZT17 was used for histological analysis. Aortic vascular remodeling is shown with representative images, scale bar = 20 μm. (**M**) Representative aortic cross sections were stained with hematoxylin and eosin (H&E) and aortic wall thickness, an index of medial hypertrophy, was measured (**J**). Changes in wall thickness are indicated with a black line. (**N**) Representative aortic sections were stained with Masson's Trichrome and (**K**) fibrosis was quantified in the 4 groups of mice. (**O**) Representative aortic cross sections were stained with Picrosirius red. (**P**) Picrosirius red stained sections were examined under polarized light for (**L**) quantification of collagen I and III content. Two-way ANOVA was used to compare diet and time of feeding (n = 4–6, $^{*}P < 0.05$).

Figure 4. TRF reduces measures of kidney damage in HFD mice. Representative histological images, quantitative histological scoring of kidney damage, medullary fibronectin gene expression, representative immunohistochemical images and quantitative analyses of kidney immune cells as well as urinary excretion of kidney damage markers or urinary excretion of oxidative stress markers in ND, ND+TRF, HFD, and HFD+TRF mice. Representative images and scoring of kidney medullary vasa recta region sections, (**A**) Masson's trichrome staining (**B**) fibrosis histological scores (**C**) Picrosirius red staining under polarized light (**D**) quantitation of collagen I and III content (**E**) Picrosirius red staining under brightfield light. Arrows indicate vasa recta fibrosis in (**A**) and (**E**). (**F**) kidney medullary fibronectin mRNA expression. Representative images of kidney cortex sections, (**G**) Masson's trichrome staining (**H**) proximal tubule vacuole scores (**I**) proximal tubule dilation scores (**J**) Picrosirius red staining under brightfield light (**K**) glomerulosclerosis histological scores (**L**) Periodic acid Schiff hematoxylin-staining (**M**) proximal tubule brush border integrity scores. Arrows indicate proximal tubule brush border in (**M**). Representative images of medullary vasa recta region with immunohistochemical staining for (**N**) CD3+ cells and (**P**) F4/80+ cells. Scale bar = 50 μm. Brown staining indicates CD3+ cells and F4/80+ cells. Quantitative analysis of (**O**) $CD3^+$ cells per medullary vasa recta bed and (**Q**) $F4/80^+$ cells per medullary vasa recta bed. Scale bar = 50 μm. Two-way ANOVA was used to compare diet and time of feeding with Tukey's posthoc test for histological scoring assessments (n = 5–13, $^*P < 0.05$). Light and dark phase (12 hour) urinary excretion of kidney damage markers, (**R**) NGAL, (**S**) KIM-1, and (**T**) albumin, from ND, ND+TRF, HFD, and HFD+TRF mice. Three-way repeated measures ANOVA was used to compare diet, time of feeding, and time of day (n = 5–12, $^*P < 0.05$). Light and dark phase (12 hour) urinary excretion of oxidative stress markers, (**U**) H_2O_2 and (**V**) 8-OHdG, from HFD and HFD+TRF mice. Two-way ANOVA was used to compare time of day and time of feeding with Sidak's post hoc test (n = 4–9, $^*P < 0.05$).

Table 1. Thoracic aortic ring vasodilator and vasoconstrictor responses during light and dark phases

	ND	ND+TRF	HFD	HFD+TRF
Light phase				
Ach-induced relaxation (% of PE)				
E_{max}	92.9 ± 1.4	85.8 ± 3.8	57.1 ± 13.9†	78.9 ± 4.0*
$logEC_{50}$	–7.14 ± 0.18	–7.07 ± 0.26	–6.69 ± 0.31†	–7.01 ± 0.10
SNP-induced relaxation (% of PE)				
E_{max}	102.4 ± 0.8	98.9 ± 0.7	104.4 ± 1.8	105.5 ± 2.3
$logEC_{50}$	–7.62 ± 0.12	–7.79 ± 0.18	–7.46 ± 0.19	–7.41 ± 0.14
PE-induced constriction (% of KCl)				
E_{max}	33.5 ± 10.5	46.1 ± 5.2	36.7 ± 6.0	58.9 ± 8.6
$logEC_{50}$	–6.09 ± 0.05	–5.68 ± 0.22$^{£}$	–5.96 ± 0.16†	–6.23 ± 0.08*
AUC	52.0 ± 15.7	64.9 ± 11.6	81.3 ± 24.0	100.5 ± 17.5
KCl-induced constriction (% Increase in Force)				
E_{max}	77.8 ± 3.7	88.2 ± 5.1	86.0 ± 7.7	84.2 ± 7.0
$logEC_{50}$	–5.56 ± 0.10	–5.63 ± 0.03	–5.87 ± 0.18	–5.70 ± 0.10
AUC	85.8 ± 6.8‡	107.1 ± 6.7	132.5 ± 19.7	113.9 ± 14.4
Dark phase				
Ach-induced relaxation (% of PE)				
E_{max}	90.4 ± 1.1	81.6 ± 3.9	93.5 ± 1.1	91.6 ± 1.7
$logEC_{50}$	–7.55 ± 0.14	–7.47 ± 0.15	–7.55 ± 0.15	–7.21 ± 0.12
SNP-induced relaxation, (% of PE)				
E_{max}	100.1 ± 0.6	101.0 ± 0.7	99.1 ± 1.6	101.6 ± 1.0
$logEC_{50}$	–7.45 ± 0.09	–7.45 ± 0.18	–7.62 ± 0.04	–7.47 ± 0.06
PE-induced constriction (% of KCl)				
E_{max}	73.7 ± 6.9	67.2 ± 13.3	53.5 ± 7.4	64.4 ± 11.0
$logEC_{50}$	–6.35 ± 0.09	–6.48 ± 0.04	–6.40 ± 0.04	–6.25 ± 0.03
AUC	135.9 ± 15.7	129.6 ± 27.7	98.7 ± 14.3	111.4 ± 19.1
KCl-induced constriction (% Increase in Force)				
E_{max}	94.7 ± 2.4	104.5 ± 4.2	102.0 ± 9.1	97.6 ± 1.5
$logEC_{50}$	–5.80 ± 0.09	–5.75 ± 0.06	–5.86 ± 0.05	–5.70 ± 0.04
AUC	129.8 ± 8.0	140.0 ± 10.2	143.1 ± 16.3	125.0 ± 2.2

Values are mean ± SEM; *n* = 5–10.
$^{\dagger}P < 0.05$ vs. HFD dark phase
*$P < 0.05$ vs. HFD light phase
$^{‡}P < 0.05$ vs. ND dark phase
$^{£}P < 0.05$ vs. ND+TRF dark phase

References

1. St-Onge M-P, Ard J, Baskin Monica L, Chiuve Stephanie E, Johnson Heather M, Kris-Etherton P, et al. Meal Timing and Frequency: Implications for Cardiovascular Disease Prevention: A Scientific Statement From the American Heart Association. *Circulation.* 2017;135(9):e96-e121.
2. Barclay JL, Husse J, Bode B, Naujokat N, Meyer-Kovac J, Schmid SM, et al. Circadian desynchrony promotes metabolic disruption in a mouse model of shiftwork. *PloS one.* 2012;7(5):e37150.
3. Scheer FAJL, Hilton MF, Mantzoros CS, and Shea SA. Adverse metabolic and cardiovascular consequences of circadian misalignment. *Proc Natl Acad Sci.* 2009;106(11):4453-4458.
4. Martino Tami A, Tata N, Belsham Denise D, Chalmers J, Straume M, Lee P, et al. Disturbed Diurnal Rhythm Alters Gene Expression and Exacerbates Cardiovascular Disease With Rescue by Resynchronization. *Hypertension.* 2007;49(5):1104-1113.
5. Honma K, Hikosaka M, Mochizuki K, and Goda T. Loss of circadian rhythm of circulating insulin concentration induced by high-fat diet intake is associated with disrupted rhythmic expression of circadian clock genes in the liver. *Metabolism.* 2016;65(4):482-491.
6. Cunningham PS, Ahern SA, Smith LC, da Silva Santos CS, Wager TT, and Bechtold DA. Targeting of the circadian clock via CK1δ/ε to improve glucose homeostasis in obesity. *Scientific Reports.* 2016;6(1):29983.
7. Kohsaka A, Laposky AD, Ramsey KM, Estrada C, Joshu C, Kobayashi Y, et al. High-fat diet disrupts behavioral and molecular circadian rhythms in mice. *Cell Metabolism.* 2007;6(5):414-421.
8. Ma L, Ma S, He H, Yang D, Chen X, Luo Z, et al. Perivascular fat-mediated vascular dysfunction and remodeling through the AMPK/mTOR pathway in high-fat diet-induced obese rats. *Hypertension Research.* 2010;33(5):446-453.

9. Santana ABC, Souza Oliveira TCd, Bianconi BL, Barauna VG, Santos EWCO, Alves TP, et al. Effect of High-Fat Diet upon Inflammatory Markers and Aortic Stiffening in Mice. *BioMed Research International.* 2014;2014:914102.

10. Jiang T, Wang Z, Proctor G, Moskowitz S, Liebman SE, Rogers T, et al. Diet-induced obesity in C57BL/6J mice causes increased renal lipid accumulation and glomerulosclerosis via a sterol regulatory element-binding protein-1c-dependent pathway. *J Biol Chem.* 2005;280(37):32317-32325.

11. Sun Y, Ge X, Li X, He J, Wei X, Du J, et al. High-fat diet promotes renal injury by inducing oxidative stress and mitochondrial dysfunction. *Cell Death & Disease.* 2020;11(10):914.

12. Millar-Craig M, Bishop C, and Raftery EB. Circadian variation of blood pressure. *The Lancet.* 1978;311(8068):795-797.

13. Otto Maria E, Svatikova A, Barretto Rodrigo Bellio de M, Santos S, Hoffmann M, Khandheria B, et al. Early Morning Attenuation of Endothelial Function in Healthy Humans. *Circulation.* 2004;109(21):2507-2510.

14. Panza JA, Epstein SE, and Quyyumi AA. Circadian Variation in Vascular Tone and Its Relation to α-Sympathetic Vasoconstrictor Activity. *New England Journal of Medicine.* 1991;325(14):986-990.

15. Liu M, Takahashi H, Morita Y, Maruyama S, Mizuno M, Yuzawa Y, et al. Non-dipping is a potent predictor of cardiovascular mortality and is associated with autonomic dysfunction in haemodialysis patients. *Nephrology Dialysis Transplantation.* 2003;18(3):563-569.

16. Denniff M, Turrell HE, Vanezis A, and Rodrigo GC. The time-of-day variation in vascular smooth muscle contractility depends on a nitric oxide signalling pathway. *Journal of Molecular and Cellular Cardiology.* 2014;66:133-140.

17. Keskil Z, Görgün CZ, Hodoglugil U, and Zengil H. Twenty-Four-Hour Variations in the Sensitivity of Rat Aorta to Vasoactive Agents. *Chronobiology International.* 1996;13(6):465-475.

18. Shaw James A, Chin-Dusting Jaye PF, Kingwell Bronwyn A, and Dart Anthony M. Diurnal Variation in Endothelium-Dependent Vasodilatation Is Not Apparent in Coronary Artery Disease. *Circulation.* 2001;103(6):806-812.

19. Kobayasi R, Akamine EH, Davel AP, Rodrigues MA, Carvalho CR, and Rossoni LV. Oxidative stress and inflammatory mediators contribute to endothelial dysfunction in high-fat diet-induced obesity in mice. *Journal of Hypertension.* 2010;28(10):2111-2119.

20. Yu Y, Rajapakse AG, Montani JP, Yang Z, and Ming XF. p38 mitogen-activated protein kinase is involved in arginase-II-mediated eNOS-uncoupling in obesity. *Cardiovasc Diabetol.* 2014;13:113.

21. García-Prieto CF, Hernández-Nuño F, Rio DD, Ruiz-Hurtado G, Aránguez I, Ruiz-Gayo M, et al. High-fat diet induces endothelial dysfunction through a down-regulation of the endothelial AMPK-PI3K-Akt-eNOS pathway. *Mol Nutr Food Res.* 2015;59(3):520-532.

22. Vogel RA, Corretti MC, and Plotnick GD. Effect of a single high-fat meal on endothelial function in healthy subjects. *Am J Cardiol.* 1997;79(3):350-354.

23. Dow CA, Stauffer BL, Greiner JJ, and DeSouza CA. Influence of habitual high dietary fat intake on endothelium-dependent vasodilation. *Appl Physiol Nutr Metab.* 2015;40(7):711-715.

24. Sutton EF, Beyl R, Early KS, Cefalu WT, Ravussin E, and Peterson CM. Early Time-Restricted Feeding Improves Insulin Sensitivity, Blood Pressure, and Oxidative Stress Even without Weight Loss in Men with Prediabetes. *Cell Metabolism.* 2018;27(6):1212-1221.

25. Jamshed H, Beyl RA, Della Manna DL, Yang ES, Ravussin E, and Peterson CM. Early Time-Restricted Feeding Improves 24-Hour Glucose Levels and Affects Markers of the Circadian Clock, Aging, and Autophagy in Humans. *Nutrients.* 2019;11(6): 1234.

26. Hutchison AT, Regmi P, Manoogian ENC, Fleischer JG, Wittert GA, Panda S, et al. Time-Restricted Feeding Improves Glucose Tolerance in Men at Risk for Type 2 Diabetes: A Randomized Crossover Trial. *Obesity (Silver Spring).* 2019;27(5):724-732.

27. Gabel K, Hoddy KK, Haggerty N, Song J, Kroeger CM, Trepanowski JF, et al. Effects of 8-hour time restricted feeding on body weight and metabolic disease risk factors in obese adults: A pilot study. *Nutrition and Healthy Aging.* 2018;4(4):345-353.

28. Wilkinson MJ, Manoogian ENC, Zadourian A, Lo H, Fakhouri S, Shoghi A, et al. Ten-Hour Time-Restricted Eating Reduces Weight, Blood Pressure, and Atherogenic Lipids in Patients with Metabolic Syndrome. *Cell Metabolism.* 2020;31(1):92-104.

29. McAllister MJ, Pigg BL, Renteria LI, and Waldman HS. Time-restricted feeding improves markers of cardiometabolic health in physically active college-age men: a 4-week randomized pre-post pilot study. *Nutrition Research.* 2020;75:32-43.

30. Salgado-Delgado R, Angeles-Castellanos M, Saderi N, Buijs RM, and Escobar C. Food Intake during the Normal Activity Phase Prevents Obesity and Circadian Desynchrony in a Rat Model of Night Work. *Endocrinology.* 2010;151(3):1019-1029.

31. Hatori M, Vollmers C, Zarrinpar A, DiTacchio L, Bushong Eric A, Gill S, et al. Time-Restricted Feeding without Reducing Caloric Intake Prevents Metabolic Diseases in Mice Fed a High-Fat Diet. *Cell Metabolism.* 2012;15(6):848-860.

32. Chaix A, Zarrinpar A, Miu P, and Panda S. Time-restricted feeding is a preventative and therapeutic intervention against diverse nutritional challenges. *Cell Metabolism.* 2014;20(6):991-1005.

33. de Goede P, Foppen E, Ritsema W, Korpel NL, Yi CX, and Kalsbeek A. Time-Restricted Feeding Improves Glucose Tolerance in Rats, but Only When in Line With the Circadian Timing System. *Front Endocrinol (Lausanne).* 2019;10:554.

34. Sherman H, Genzer Y, Cohen R, Chapnik N, Madar Z, and Froy O. Timed high-fat diet resets circadian metabolism and prevents obesity. *FASEB J.* 2012;26(8):3493-3502.

35. Chaix A, Lin T, Le HD, Chang MW, and Panda S. Time-Restricted Feeding Prevents Obesity and Metabolic Syndrome in Mice Lacking a Circadian Clock. *Cell Metabolism.* 2019;29(2):303-319.

36. O'Connor SG, Boyd P, Bailey CP, Shams-White MM, Agurs-Collins T, Hall K, et al. Perspective: Time-Restricted Eating Compared with Caloric Restriction: Potential Facilitators and Barriers of Long-Term Weight Loss Maintenance. *Advances in Nutrition.* 2021;12(2):325-333.

37. Adamek A, and Kasprzak A. Insulin-Like Growth Factor (IGF) System in Liver Diseases. *Int J Mol Sci.* 2018;19(5):1308.

38. Puchalska P, and Crawford PA. Multi-dimensional Roles of Ketone Bodies in Fuel Metabolism, Signaling, and Therapeutics. *Cell Metabolism.* 2017;25(2):262-284.

39. Sansbury Brian E, Cummins Timothy D, Tang Y, Hellmann J, Holden Candice R, Harbeson Matthew A, et al. Overexpression of Endothelial Nitric Oxide Synthase Prevents Diet-Induced Obesity and Regulates Adipocyte Phenotype. *Circulation Research.* 2012;111(9):1176-1189.

40. Huang K, Huang Y, Frankel J, Addis C, Jaswani L, Wehner PS, et al. The short-term consumption of a moderately high-fat diet alters nitric oxide bioavailability in lean female Zucker rats. *Can J Physiol Pharmacol.* 2011;89(4):245-257.

41. Lauer T, Preik M, Rassaf T, Strauer BE, Deussen A, Feelisch M, et al. Plasma nitrite rather than nitrate reflects regional endothelial nitric oxide synthase activity but lacks intrinsic vasodilator action. *Proc Natl Acad Sci.* 2001;98(22):12814-12819.

42. Maas R, Xanthakis V, Göen T, Müller J, Schwedhelm E, Böger RH, et al. Plasma Nitrate and Incidence of Cardiovascular Disease and All-Cause Mortality in the Community: The Framingham Offspring Study. *Journal of the American Heart Association.*6(11):e006224.

43. Lembo G, Vecchione C, Fratta L, Marino G, Trimarco V, Amati G, et al. Leptin induces direct vasodilation through distinct endothelial mechanisms. *Diabetes.* 2000;49(2):293.

44. Kimura K, Tsuda K, Baba A, Kawabe T, Boh-oka S, Ibata M, et al. Involvement of nitric oxide in endothelium-dependent arterial relaxation by leptin. *Biochem Biophys Res Commun.* 2000;273(2):745-749.

45. Knudson JD, Dincer UD, Zhang C, Swafford AN, Jr., Koshida R, Picchi A, et al. Leptin receptors are expressed in coronary arteries, and hyperleptinemia causes significant coronary endothelial dysfunction. *Am J Physiol: Heart Circ Physiol.* 2005;289(1):H48-56.

46. Korda M, Kubant R, Patton S, and Malinski T. Leptin-induced endothelial dysfunction in obesity. *Am J Physiol: Heart Circ Physiol.* 2008;295(4):H1514-1521.

47. Belin de Chantemèle Eric J, Mintz James D, Rainey William E, and Stepp David W. Impact of Leptin-Mediated Sympatho-Activation on Cardiovascular Function in Obese Mice. *Hypertension.* 2011;58(2):271-279.

48. Morioka T, Emoto M, Yamazaki Y, Kawano N, Imamura S, Numaguchi R, et al. Leptin is associated with vascular endothelial function in overweight patients with type 2 diabetes. *Cardiovascular Diabetology.* 2014;13(1):10.

49. Deng G, Long Y, Yu YR, and Li MR. Adiponectin directly improves endothelial dysfunction in obese rats through the AMPK-eNOS Pathway. *Int J Obes (Lond).* 2010;34(1):165-171.

50. Ouchi N, Ohishi M, Kihara S, Funahashi T, Nakamura T, Nagaretani H, et al. Association of hypoadiponectinemia with impaired vasoreactivity. *Hypertension.* 2003;42(3):231-4.

51. Ouedraogo R, Gong Y, Berzins B, Wu X, Mahadev K, Hough K, et al. Adiponectin deficiency increases leukocyte-endothelium interactions via upregulation of endothelial cell adhesion molecules in vivo. *J Clin Invest.* 2007;117(6):1718-1726.

52. Deji N, Kume S, Araki S-i, Soumura M, Sugimoto T, Isshiki K, et al. Structural and functional changes in the kidneys of high-fat diet-induced obese mice. *Am J Physiol: Renal Physiol.* 2009;296(1):F118-F126.

53. Calligaris SD, Lecanda M, Solis F, Ezquer M, Gutiérrez J, Brandan E, et al. Mice Long-Term High-Fat Diet Feeding Recapitulates Human Cardiovascular Alterations: An Animal Model to Study the Early Phases of Diabetic Cardiomyopathy. *PloS one.* 2013;8(4):e60931.

54. Chaar LJ, Coelho A, Silva NM, Festuccia WL, and Antunes VR. High-fat diet-induced hypertension and autonomic imbalance are associated with an upregulation of CART in the dorsomedial hypothalamus of mice. *Physiological Reports.* 2016;4(11):e12811.

55. Bruder-Nascimento T, Ekeledo OJ, Anderson R, Le HB, and Belin de Chantemèle EJ. Long Term High Fat Diet Treatment: An Appropriate Approach to Study the Sex-Specificity of the Autonomic and Cardiovascular Responses to Obesity in Mice. *Frontiers in Physiology.* 2017;8(32).

56. Su W, Guo Z, Randall DC, Cassis L, Brown DR, and Gong MC. Hypertension and disrupted blood pressure circadian rhythm in type 2 diabetic db/db mice. *Am J Physiol: Heart Circ Physiol.* 2008;295(4):H1634-41.

57. Goncalves AC, Tank J, Diedrich A, Hilzendeger A, Plehm R, Bader M, et al. Diabetic hypertensive leptin receptor-deficient db/db mice develop cardioregulatory autonomic dysfunction. *Hypertension.* 2009;53(2):387-92.

58. Pistrosch F, Reissmann E, Wildbrett J, Koehler C, and Hanefeld M. Relationship between diurnal blood pressure variation and diurnal blood glucose levels in type 2 diabetic patients. *American Journal of Hypertension.* 2007;20(5):541-5.

59. Kim Y-S, Davis SCAT, Stok WJ, van Ittersum FJ, and van Lieshout JJ. Impaired nocturnal blood pressure dipping in patients with type 2 diabetes mellitus. *Hypertension Research.* 2019;42(1):59-66.

60. Verdecchia P, Porcellati C, Schillaci G, Borgioni C, Ciucci A, Battistelli M, et al. Ambulatory blood pressure. An independent predictor of prognosis in essential hypertension. *Hypertension.* 1994;24(6):793-801.

61. Intengan Hope D, and Schiffrin Ernesto L. Vascular Remodeling in Hypertension. *Hypertension.* 2001;38(3):581-7.

62. Bidani Anil K, and Griffin Karen A. Pathophysiology of Hypertensive Renal Damage. *Hypertension.* 2004;44(5):595-601.

63. Pereira LMM, Bezerra DG, and Mandarim-de-Lacerda CA. Aortic wall remodeling in rats with nitric oxide deficiency treated by enalapril or verapamil. *Pathology - Research and Practice.* 2004;200(3):211-7.

64. Hayakawa H, and Raij L. The link among nitric oxide synthase activity, endothelial function, and aortic and ventricular hypertrophy in hypertension. *Hypertension.* 1997;29(1 Pt 2):235-41.

65. Gibbons GH. Endothelial function as a determinant of vascular function and structure: A new therapeutic target. *The American Journal of Cardiology.* 1997;79(5, Supplement 1):3-8.

66. Vanhoutte PM, Shimokawa H, Tang EHC, and Feletou M. Endothelial dysfunction and vascular disease. *Acta Physiologica.* 2009;196(2):193-222.

67. Cai H, and Harrison DG. Endothelial Dysfunction in Cardiovascular Diseases: The Role of Oxidant Stress. *Circulation Research.* 2000;87(10):840-4.

68. Bauer J, Ripperger A, Frantz S, Ergün S, Schwedhelm E, and Benndorf RA. Pathophysiology of isoprostanes in the cardiovascular system: implications of isoprostane-mediated thromboxane A2 receptor activation. *Br J Pharmacol.* 2014;171(13):3115-31.

69. Sutton EF, Beyl R, Early KS, Cefalu WT, Ravussin E, and Peterson CM. Early Time-Restricted Feeding Improves Insulin Sensitivity, Blood Pressure, and Oxidative Stress Even without Weight Loss in Men with Prediabetes. *Cell Metabolism.* 2018;27(6):1212-21 e3.

70. Mastronardi CA, Yu WH, and McCann SM. Resting and circadian release of nitric oxide is controlled by leptin in male rats. *Proc Natl Acad Sci.* 2002;99(8):5721.

71. Jonvik KL, Nyakayiru J, Pinckaers PJM, Senden JMG, van Loon LJC, and Verdijk LB. Nitrate-Rich Vegetables Increase Plasma Nitrate and Nitrite Concentrations and Lower Blood Pressure in Healthy Adults. *The Journal of Nutrition.* 2016;146(5):986-993.

72. Miller GD, Marsh AP, Dove RW, Beavers D, Presley T, Helms C, et al. Plasma nitrate and nitrite are increased by a high-nitrate supplement but not by high-nitrate foods in older adults. *Nutr Res.* 2012;32(3):160-8.

73. Su W, Xie Z, Guo Z, Duncan MJ, Lutshumba J, and Gong MC. Altered clock gene expression and vascular smooth muscle diurnal contractile variations in type 2 diabetic db/db mice. *Am J Physiol: Heart Circ Physiol.* 2011;302(3):H621-H33.

74. Denniff M, Turrell HE, Vanezis A, and Rodrigo GC. The time-of-day variation in vascular smooth muscle contractility depends on a nitric oxide signalling pathway. *J Mol Cell Cardiol.* 2014;66:133-40.

75. Conti V, Russomanno G, Corbi G, Izzo V, Vecchione C, and Filippelli A. Adrenoreceptors and nitric oxide in the cardiovascular system. *Front Physiol.* 2013;4:321.

76. Serra A, Romero R, Lopez D, Navarro M, Esteve A, Perez N, et al. Renal injury in the extremely obese patients with normal renal function. *Kidney Int.* 2008;73(8):947-55.

77. Jang H-S, Noh MR, Kim J, and Padanilam BJ. Defective Mitochondrial Fatty Acid Oxidation and Lipotoxicity in Kidney Diseases. *Front Med (Lausanne).* 2020;7:65.

78. Kume S, Uzu T, Araki S, Sugimoto T, Isshiki K, Chin-Kanasaki M, et al. Role of altered renal lipid metabolism in the development of renal injury induced by a high-fat diet. *J Am Soc Nephrol.* 2007;18(10):2715-23.

79. Laurentius T, Raffetseder U, Fellner C, Kob R, Nourbakhsh M, Floege J, et al. High-fat diet-induced obesity causes an inflammatory microenvironment in the kidneys of aging Long-Evans rats. *Journal of Inflammation.* 2019;16(1):14.

80. Stemmer K, Perez-Tilve D, Ananthakrishnan G, Bort A, Seeley RJ, Tschöp MH, et al. High-fat-diet-induced obesity causes an inflammatory and tumor-promoting microenvironment in the rat kidney. *Disease Models & Mechanisms.* 2012;5(5):627.

81. Dumas SJ, Meta E, Borri M, Luo Y, Li X, Rabelink TJ, et al. Phenotypic diversity and metabolic specialization of renal endothelial cells. *Nature Reviews Nephrology.* 2021;17(7):441-464.

82. van der Heijden RA, Bijzet J, Meijers WC, Yakala GK, Kleemann R, Nguyen TQ, et al. Obesity-induced chronic inflammation in high fat diet challenged C57BL/6J mice is associated with acceleration of age-dependent renal amyloidosis. *Scientific Reports.* 2015;5(1):16474.

83. Schmidt-Ott KM. Neutrophil gelatinase-associated lipocalin as a biomarker of acute kidney injury--where do we stand today? *Nephrol Dial Transplant.* 2011;26(3):762-4.

84. Zhang Y, Yuan M, Bradley Katherine M, Dong F, Anversa P, and Ren J. Insulin-Like Growth Factor 1 Alleviates High-Fat Diet–Induced Myocardial Contractile Dysfunction. *Hypertension.* 2012;59(3):680-93.

85. Chakraborty S, Galla S, Cheng X, Yeo J-Y, Mell B, Singh V, et al. Salt-Responsive Metabolite, β-Hydroxybutyrate, Attenuates Hypertension. *Cell Rep.* 2018;25(3):677-89.e4.

86. García-Gaytán AC, Miranda-Anaya M, Turrubiate I, López-De Portugal L, Bocanegra-Botello GN, López-Islas A, et al. Synchronization of the circadian clock by time-restricted feeding with progressive increasing calorie intake. Resemblances and differences regarding a sustained hypocaloric restriction. *Scientific Reports.* 2020;10(1):10036.

87. Mey JT, Erickson ML, Axelrod CL, King WT, Flask CA, McCullough AJ, et al. β-Hydroxybutyrate is reduced in humans with obesity-related NAFLD and displays a dose-dependent effect on skeletal muscle mitochondrial respiration in vitro. *Am J Physiol Endocrinol Metab.* 2020;319(1):E187-e95.

88. Poetsch MS, Strano A, and Guan K. Role of Leptin in Cardiovascular Diseases. *Frontiers in Endocrinology.* 2020;11:354-.

89. Anea CB, Zhang M, Stepp DW, Simkins GB, Reed G, Fulton DJ, et al. Vascular disease in mice with a dysfunctional circadian clock. *Circulation.* 2009;119(11):1510-7.

90. Anea CB, Cheng B, Sharma S, Kumar S, Caldwell RW, Yao L, et al. Increased superoxide and endothelial NO synthase uncoupling in blood vessels of Bmal1-knockout mice. *Circulation research.* 2012;111(9):1157-65.

91. Viswambharan H, Carvas JM, Antic V, Marecic A, Jud C, Zaugg CE, et al. Mutation of the circadian clock gene Per2 alters vascular endothelial function. *Circulation.* 2007;115(16):2188-95.

92. Westgate E, Cheng Y, Reilly D, Price T, Walisser J, Bradfield C, et al. Genetic Components of the Circadian Clock Regulate Thrombogenesis In Vivo. *Circulation.* 2008;117:2087-95.

93. Xie Z, Su W, Liu S, Zhao G, Esser K, Schroder EA, et al. Smooth-muscle BMAL1 participates in blood pressure circadian rhythm regulation. *J Clin Invest.* 2015;125(1):324-36.

94. Bhatwadekar AD, Beli E, Diao Y, Chen J, Luo Q, Alex A, et al. Conditional Deletion of Bmal1 Accentuates Microvascular and Macrovascular Injury. *Am J Pathol.* 2017;187(6):1426-35.

95. Bray MS, Ratcliffe WF, Grenett MH, Brewer RA, Gamble KL, and Young ME. Quantitative analysis of light-phase restricted feeding reveals metabolic dyssynchrony in mice. *Int J Obes (Lond).* 2013;37(6):843-52.

96. Mia S, Sonkar R, Williams L, Latimer MN, Frayne Robillard I, Diwan A, et al. Impact of obesity on day-night differences in cardiac metabolism. *FASEB J.* 2021;35(3):e21298.

97. Dériaz O, Fournier G, Tremblay A, Després JP, and Bouchard C. Lean-body-mass composition and resting energy expenditure before and after long-term overfeeding. *The American Journal of Clinical Nutrition.* 1992;56(5):840-7.

98. Taicher GZ, Tinsley FC, Reiderman A, and Heiman ML. Quantitative magnetic resonance (QMR) method for bone and whole-body-composition analysis. *Analytical and Bioanalytical Chemistry.* 2003;377(6):990-1002.

99. Fox BM, Becker BK, Loria AS, Hyndman KA, Jin C, Clark H, et al. Acute Pressor Response to Psychosocial Stress Is Dependent on Endothelium-Derived Endothelin-1. *J Am Heart Assoc.* 2018;7(4):e007863.

100. Boesen EI, Sasser JM, Saleh MA, Potter WA, Woods M, Warner TD, et al. Interleukin-1beta, but not interleukin-6, enhances renal and systemic endothelin production in vivo. *Am J Physiol Renal Physiol.* 2008;295(2):F446-F53.

101. Zhang D, Jin C, Obi IE, Rhoads MK, Soliman RH, Sedaka RS, et al. Loss of circadian gene Bmal1 in the collecting duct lowers blood pressure in male, but not female, mice. *Am J Physiol Renal Physiol.* 2020.

102. Ho DH, Burch ML, Musall B, Musall JB, Hyndman KA, and Pollock JS. Early life stress in male mice induces superoxide production and endothelial dysfunction in adulthood. *Am J Physiol: Heart Circ Physiol.* 2016;310(9):H1267-H74.

103. Hyndman KA, Boesen EI, Elmarakby AA, Brands MW, Huang P, Kohan DE, et al. Renal collecting duct NOS1 maintains fluid-electrolyte homeostasis and blood pressure. *Hypertension.* 2013;62(1):91-8.

104. Kang KT, Sullivan JC, Sasser JM, Imig JD, and Pollock JS. Novel nitric oxide synthase--dependent mechanism of vasorelaxation in small arteries from hypertensive rats. *Hypertension.* 2007;49(4):893-901.

105. Loria AS, Spradley FT, Obi IE, Becker BK, Miguel CD, Speed JS, et al. Maternal separation enhances anticontractile perivascular adipose tissue function in male rats on a high-fat diet. *Am J Physiol: Regu, Integr, Comp Physiol.* 2018;315(6):R1085-R95.

106. Spradley FT, Ho DH, and Pollock JS. Dahl SS rats demonstrate enhanced aortic perivascular adipose tissue-mediated buffering of vasoconstriction through activation of NOS in the endothelium. *Am J Physiol: Regu, Integr, Comp Physiol.* 2016;310(3):R286-R96.

107. Sullivan JC, Loomis ED, Collins M, Imig JD, Inscho EW, and Pollock JS. Age-related alterations in NOS and oxidative stress in mesenteric arteries from male and female rats. *Journal of Applied Physiology.* 2004;97(4):1268-74.

108. Oller J, Méndez-Barbero N, Ruiz EJ, Villahoz S, Renard M, Canelas LI, et al. Nitric oxide mediates aortic disease in mice deficient in the metalloprotease Adamts1 and in a mouse model of Marfan syndrome. *Nature Medicine.* 2017;23(2):200-12.

109. Grigorova YN, Juhasz O, Zernetkina V, Fishbein KW, Lakatta EG, Fedorova OV, et al. Aortic Fibrosis, Induced by High Salt Intake in the Absence of Hypertensive Response, Is Reduced by a Monoclonal Antibody to Marinobufagenin. *Am J Hyper.* 2016;29(5):641-6.

110. De Miguel C, Sedaka R, Kasztan M, Lever JM, Sonnenberger M, Abad A, et al. Tauroursodeoxycholic acid (TUDCA) abolishes chronic high salt-induced renal injury and inflammation. *Acta Physiologica.* 2019;226(1):e13227.

111. Kasztan M, Fox BM, Speed JS, De Miguel C, Gohar EY, Townes TM, et al. Long-Term Endothelin-A Receptor Antagonism Provides Robust Renal Protection in Humanized Sickle Cell Disease Mice. *J Am Soc Nephrol.* 2017;28(8):2443-58.

112. Zhang D, Colson JC, Jin C, Becker BK, Rhoads MK, Pati P, et al. Timing of Food Intake Drives the Circadian Rhythm of Blood Pressure. *Function (Oxf).* 2021;2(1):zqaa034.

113. Hyndman KA, Dugas C, Arguello AM, Goodchild TT, Buckley KM, Burch M, et al. High salt induces autocrine actions of ET-1 on inner medullary collecting duct NO production via upregulated ETB receptor expression. *Am J Physiol: Regu, Integr, Comp Physiol.* 2016;311(2):R263-R71.

114. Valcin JA, Udoh US, Swain TM, Andringa KK, Patel CR, Al Diffalha S, et al. Alcohol and Liver Clock Disruption Increase Small Droplet Macrosteatosis, Alter Lipid Metabolism and Clock Gene mRNA Rhythms, and Remodel the Triglyceride Lipidome in Mouse Liver. *Frontiers in Physiology.* 2020;11(1048).